

# 3D MHD model of the collapse and fragmentation of turbulent prestellar core

Alexander E. Dudorov, and Sergey N. Zamozdra

Chelyabinsk State University, Russia  
 email: dudorov@csu.ru, sezam@csu.ru

**Abstract.** With the help of 3D MHD simulations we investigate the collapse and fragmentation of rotating turbulent prestellar core embedded into turbulent medium. The numerical code is based on a high resolution Godunov-type finite-difference scheme. Initial turbulence is represented by the ensemble of Alfvén waves with power law spectrum. Our computations show that under realistic parameters two bound fragments can appear when the density increases at  $100 - 10^3$  times. The distance between the fragments is about 0.1 of the initial core radius and their orbital period is comparable to the initial free fall time of the core. These results can explain the origin of binary stars with separation  $0.001 - 0.01$  pc in the Galaxy field.

**Keywords.** MHD, turbulence, waves, stars: formation, ISM: globules, ISM: magnetic fields

## 1. Introduction

Prestellar cores in molecular clouds are gravitationally bound condensations with stellar masses. The collapse and fragmentation of such cores lead to formation of single or multiple stars. We investigate the influence of magnetic field, rotation and turbulence on a prestellar core collapse and early fragmentation using 3D magnetohydrodynamical (MHD) simulations. Similar problem without turbulence was studied by Machida et al. (2008), Hennebelle & Teyssier (2008) and Duffin & Pudritz (2009). The role of turbulence was investigated by Price & Bate (2008) and Wang et al. (2010) for massive clouds without rotation.

We carry out low resolution simulations (with cell number  $128^3$ ) and focus the attention on initial conditions and results analysis. The computational domain contains both the core and surrounding medium to describe a turbulent energy redistribution via MHD waves propagation (see Heitsch et al. 2001). The initial pulsations amplitudes depend on density (see McKee & Zweibel 1995) because a turbulence in non-uniform medium is inhomogeneous one. A bound fragment is found with the help of internal motion separation on inward, outward and tangential components relative to fragment mass center.

## 2. Model

*Initial conditions.* Uniform spherical core with radius  $R = 0.3$  of domain size is embedded into uniform cubic medium (see fig. 1) with density  $\rho = 1/4$  of core density. Thermal pressure is balanced. Large scale magnetic field  $\vec{B}_0$  is uniform. The core and medium can rotate as solid body with axis parallel to  $\vec{B}_0$ . Turbulence is the ensemble of plane Alfvén waves with linear polarization and isotropic power law spectrum. The initial velocity pulsation  $\vec{v}_{\vec{k}}$  in the Alfvén wave with wave vector  $\vec{k}$  is directed perpendicularly to  $(\vec{k}, \vec{B}_0)$

plane and has amplitude

$$v_{\vec{k}}(\vec{r}) = Ak^{-\alpha} \rho^{\beta}(\vec{r}) \sin\left(\vec{k}\vec{r} + \varphi_{\vec{k}}\right), \quad (2.1)$$

where  $A$  is the normalization factor,  $\varphi_{\vec{k}}$  is the random phase. The magnetic pulsation is  $\vec{B}_{\vec{k}} = \mp s \vec{v}_{\vec{k}} \sqrt{\rho}$ , where  $s = \text{sign}(\vec{k}\vec{B}_0)$ .

Boundary conditions. Periodical boundary conditions are used to promote the MHD waves circulation through the medium.

Equations and methods. Ideal MHD approximation with isothermal equation of state is adopted. The simulations are carried out with the help of numerical code Megalion (Dudorov et al. 2003) that realizes the modified Lax-Friedrichs method for hyperbolic equations and conjugated gradients method for gravitation equation. The computations are single threading.

Bound fragments. A fragment is the set of contacted cells where density exceeds some level. The fragment is bound if

$$E_g + E_{in} > E_{th} + E_m + E_{tan} + E_{out}, \quad (2.2)$$

where  $E_g$  is the absolute value of gravitational energy,  $E_{th}$ ,  $E_m$  are the thermal and magnetic energies,  $E_{in}$ ,  $E_{out}$ ,  $E_{tan}$  are the energies of inward, outward and tangential motions relative to fragment mass center.

Basic parameters.

1) The ratios of thermal  $E_T$ , large scale magnetic  $E_M$ , turbulent kinetic  $E_K$  and rotational  $E_{\Omega}$  energies of the core to the absolute value of its gravitational energy  $E_G$ .

2) The index of wave spectrum:  $\alpha \in (1/4, 1/2)$ .

3) The index of  $v_{\vec{k}} - \rho$  relation:  $\beta \in (-1/2, 1/4)$ . Note that  $\beta = -1/2$  means the balance of wave pressure.

4) Maximal and minimal dimensionless wave numbers:  $n_{min} \in (2, 3)$  and  $n_{max} \in (8, 12)$ .

In all the models  $E_T/E_G = 0.1$ . The model with parameters  $E_{\Omega}/E_G = 0.05$ ,  $E_K/E_G = 0.3$ ,  $E_M/E_G = 0.3$ ,  $\alpha = 1/3$ ,  $\beta = -1/2$ ,  $n_{min} = 2$  and  $n_{max} = 8$  is called "base model".

### 3. Results

We have computed successfully 40 models. The basic results are following.

(a) Turbulence produces density pulsations almost during all the collapse. For example at fig. 2 we can see clumpy structure both at the initial and final simulation stages.

(b) Turbulence usually increases the collapse time by 5 – 10% (fig. 3). Larger  $\beta$  leads to larger collapse time because of increasing of turbulent pressure gradient. The collapse with fragmentation is more delayed than the collapse without fragmentation.

(c) During the isothermal collapse stage Jeans mass decreases and some fragments become bound. Only two bound fragments can appear when the density increases at 100 – 1000 times (fig. 4a).

(d) The magnetic field directions in the fragments differ from  $\vec{B}_0$  direction. For example in fig. 4b we can see the declinations of magnetic field at 30 – 45° from  $z$ -axis.

(e) In the absence of rotation the early fragmentation is possible when  $E_K > E_T$  and  $E_K \geq E_M$  (fig. 5 left). At moderate rotation ( $E_{\Omega}/E_G = 0.05$ ) the early fragmentation becomes possible even when  $E_K = E_T$  and  $E_K < E_M$  (fig. 5 middle). At faster rotation ( $E_{\Omega}/E_G = 0.1$ ) the early fragmentation occurs in most cases (fig. 5 right).

(f) In average, the initial total mass of the bound fragments  $\approx 0.07$  of core mass, the major to minor mass ratio  $\approx 1.5$  (fig. 6).

(g) The distance between the mass centres of the fragments is  $d = 0.13 - 0.29R$ , their orbital period is  $P = 0.47 - 3.2t_{ff}$  (fig. 7). The correlation between distance and period resembles the third Kepler law ( $P \propto d^{3/2}$ ).

(h) The properties of bound cores almost independent on initial spectral slope  $\alpha$ . This results is surprising and must be checked.

(i) Since typically  $R \simeq 0.01 - 0.1$  pc then  $d \simeq 0.001 - 0.01$  pc that corresponds to the separation in wide binary protostars and stars of the Galaxy field (see Connelley et al. 2008).

#### 4. Conclusions

We carried out 3D MHD simulations of the collapse and fragmentation of rotating turbulent prestellar core embedded into turbulent medium. We conclude that:

- under realistic parameters only two bound fragments can appear when the core density increases at 100 – 1000 times,
- the distance between such fragments is about 0.1 of the initial core radius,
- their orbital period is comparable to the initial free fall time of the core,
- these results can explain the origin of binary stars in the Galaxy field with semi-major axis in the range 0.001 – 0.01 pc.

At the next stage of the project we will use the AMR technology realized in the code Megalion. That will improve the resolution and lead to more interesting results. It is also desirable to develop the turbulent initial conditions without MHD discontinuities at the core surface.

#### References

- Machida, M.N., Tomisaka, K., Matsumoto, T., Inutsuka, S. 2008, *ApJ*, 677, 327  
 Hennebelle, P. & Teyssier, R. 2008, *A&A*, 477, 25  
 Duffin, D. & Pudritz, R. 2009, *ApJ*(Letters), 706, L46  
 Price, D.J. & Bate, M.R. 2008, *MNRAS*, 385, 1820  
 Wang, P., Li, Zhi-Yun, Abel, T. & Nakamura, F. 2010, *ApJ*, 709, 27  
 Heitsch, F., Mac Low, M. & Klessen, R.S. 2001, *ApJ*, 547, 280  
 McKee, C.F. & Zweibel, E.G. 1995, *ApJ*, 440, 686  
 Dudorov, A.E., Zhilkin, A.G., Stepanov, K.E. et al. 2003, *VII Zababakhin Scientific Talks*, Intern. conf. proceedings, <http://www.vniitf.ru/rig/konfer/7zst/reports/s6/s-6.htm>  
 Connelley, M.S., Reipurth, B. & Tokunaga, A.T. 2008, *AJ*, 135, 2526

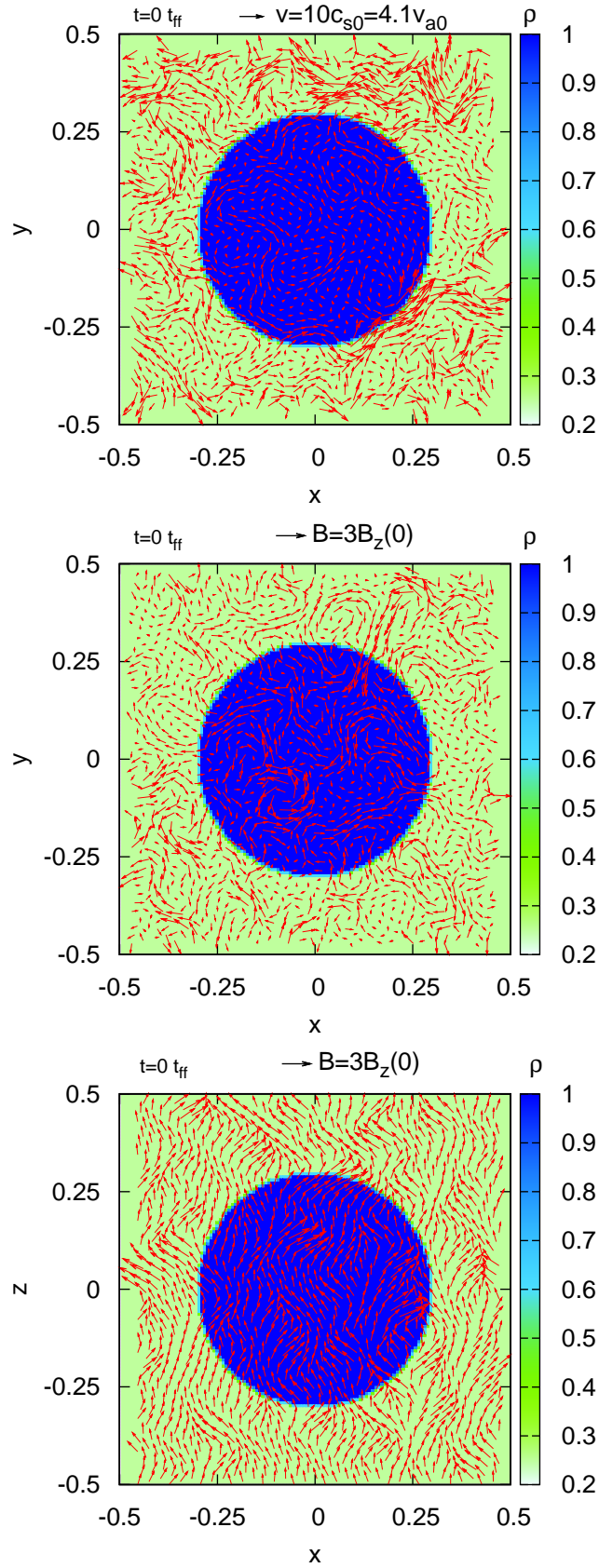


**Figure 1.** Initial distributions of density (color scale), velocity and magnetic field (arrows) at different planes in the base model.

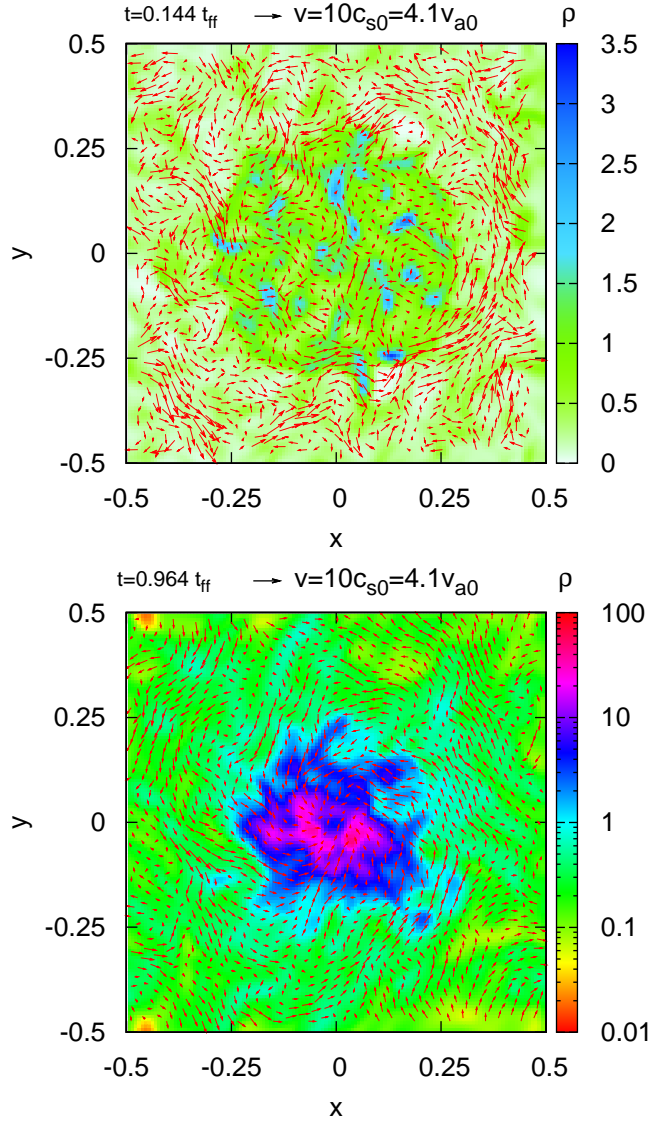


**Figure 2.** Distributions of density (color scale) and velocity (arrows) at the plane  $z=0$  in the base model at  $t=0.144t_{ff}$  and  $t=0.964t_{ff}$ .

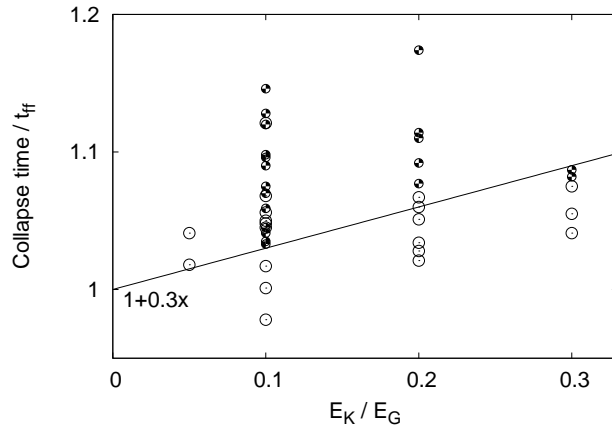


**Figure 3.** Collapse time versus  $E_K/E_G$  ratio in all 40 models. Open circles – no fragmentation, filled circles – yes. Solid line emphasizes that the collapse with fragmentation is more delayed than the collapse without fragmentation.

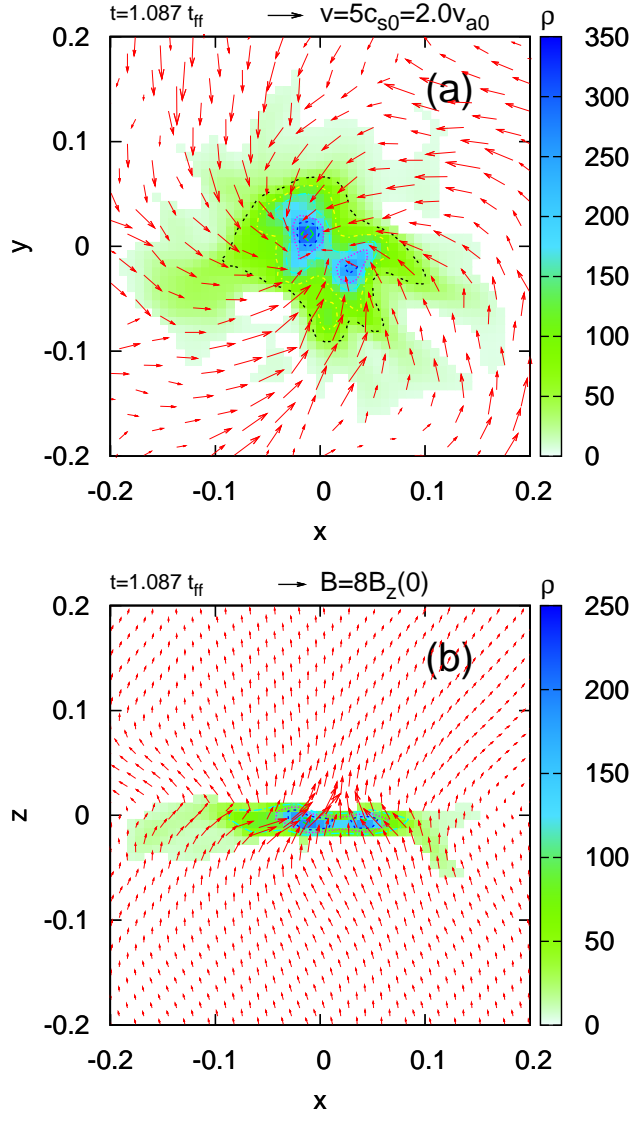


**Figure 4.** Final distributions of density and velocity at the plane  $z = 0$  (a) as well as density and magnetic field at the plane  $y = 0$  (b) in the central region of base model. Only density  $\rho > 5$  is shown (color scale and contours).

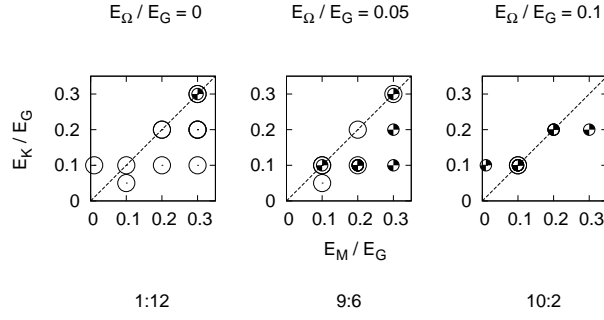


**Figure 5.** Fragmentation diagram: open circles – no, filled circles – yes. See yes-to-no ratio at the foot.

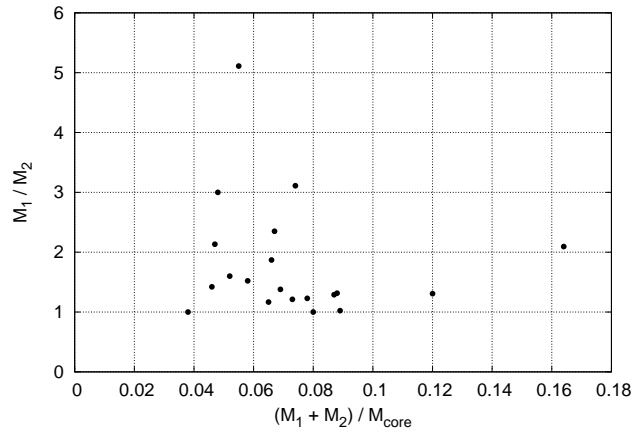


**Figure 6.** Fragments mass ratio versus their total mass to core mass ratio.



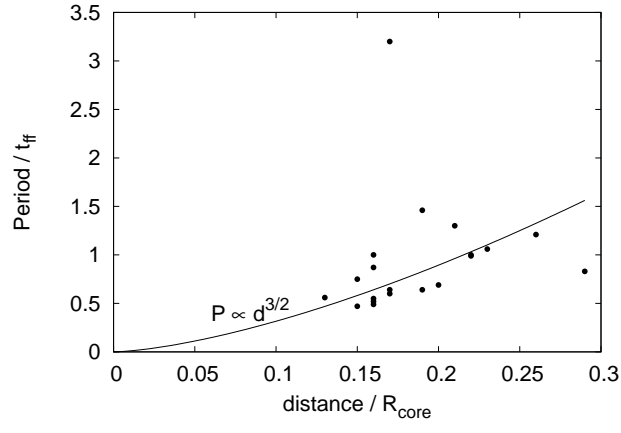


**Figure 7.** Orbital period of fragments (in core free fall time units) versus their separation to core radius ratio. The solid curve shows that the correlation between distance and period resembles the third Kepler law ( $P \propto d^{3/2}$ ).